Technical Report Documentation Page

1. Report No. FHWA/TX-08/0-5482-1	2. Government Accession No.	3. Recipient's Catalog No.
4. Title and Subtitle Literature Review on Concrete Pavement Overlays Over Existing Asphalt Pavement Structures		5. Report Date March 2007; Revised September 2008 6. Performing Organization Code
7. Author(s) Dong-Ho Kim, Mohammad R. Suliman, and Moon Won		8. Performing Organization Report No. 0-5482-1
9. Performing Organization Name and Address Center for Transportation Research The University of Texas at Austin 3208 Red River, Suite 200 Austin, TX 78705-2650		10. Work Unit No. (TRAIS) 11. Contract or Grant No. 0-5482
12. Sponsoring Agency Name and Address Texas Department of Transportation Research and Technology Implementation Office P.O. Box 5080 Austin, TX 78763-5080		13. Type of Report and Period Covered Technical Report 9/1/2005-8/31/2007 14. Sponsoring Agency Code

15. Supplementary Notes
Project performed in cooperation with the Texas Department of Transportation and the Federal Highway Administration.
Project Title: Concrete Pavement Overlays Over Existing Asphalt Pavement Structures

16. Abstract

The primary objective of this report is to summarize the findings of the literature review on the performance of whitetopping test sections and design procedures. Two questions face pavement engineers who consider using Portland cement concrete (PCC) overlays over hot mix asphalt concrete (HMAC): (1) Is the HMAC section in need of rehabilitation a good candidate for PCC overlay? (2) If it is, what should be the optimum PCC overlay structure, thin whitetopping (TWT) or full depth regular PCC pavement?

To get answers to these questions, it is important to be able to properly evaluate the existing HMAC pavement for its ability to uniformly support PCC slabs. Without the ability to properly evaluate the supporting capability of HMAC pavement, it's difficult to develop reasonable rehabilitation strategies. TxDOT developed design standards and special specification for thin white topping. However, TxDOT currently does not have guidelines or design procedures for the rehabilitation of HMAC showing rutting and shoving, with TWT.

Several whitetopping projects were constructed over the years. The performance of these projects was investigated. They include test sections in Illinois, Minnesota, and Colorado. Several design procedures for whitetopping were reviewed: 1) Colorado whitetopping design procedures; 2) the Portland Cement Association design procedure developed by the Construction Technology Laboratories; 3) American Concrete Pavement Association design procedures; 4) design procedures developed by the New Jersey DOT, which were based on theoretical analysis. Review of these design procedures reveals that improvements are still needed for the proper and accurate determination of whitetopping pavement system.

17. Key Words white topping, pavement performance, pavement rehabilitation	18. Distribution Statement No restrictions. This document is available to the public through the National Technical Information Service, Springfield, Virginia 22161; www.ntis.gov.

19. Security Classif. (of report) Unclassified	20. Security Classif. (of this page) Unclassified	21. No. of pages 60	22. Price

Form DOT F 1700.7 (8-72) Reproduction of completed page authorized

Literature Review on Concrete Pavement Overlays over Existing Asphalt Structures

Dong-Ho Kim
Mohammad R. Suliman
Moon Won

CTR Technical Report:	0-5482-1
Report Date:	March 2007; Revised September 2008
Project:	0-5482
Project Title:	Concrete Pavement Overlays Over Existing Asphalt Structures
Sponsoring Agency:	Texas Department of Transportation
Performing Agency:	Center for Transportation Research at The University of Texas at Austin

Project performed in cooperation with the Texas Department of Transportation and the Federal Highway Administration.

Center for Transportation Research
The University of Texas at Austin
3208 Red River
Austin, TX 78705

www.utexas.edu/research/ctr

Disclaimers

Author's Disclaimer: The contents of this report reflect the views of the authors, who are responsible for the facts and the accuracy of the data presented herein. The contents do not necessarily reflect the official view or policies of the Federal Highway Administration or the Texas Department of Transportation (TxDOT). This report does not constitute a standard, specification, or regulation.

Patent Disclaimer: There was no invention or discovery conceived or first actually reduced to practice in the course of or under this contract, including any art, method, process, machine manufacture, design or composition of matter, or any new useful improvement thereof, or any variety of plant, which is or may be patentable under the patent laws of the United States of America or any foreign country.

Engineering Disclaimer

NOT INTENDED FOR CONSTRUCTION, BIDDING, OR PERMIT PURPOSES.

Project Engineer: Moon Won
Professional Engineer License State and Number: Texas No. 76918
P. E. Designation: Research Supervisor

Acknowledgments

The authors express sincere appreciation to the Project Director, Tomas Saenz, who has provided valuable advices and suggestions. Also, the support received from David Head, the Program Coordinator, and German Claros, RTI Research Engineer, has been invaluable.

Table of Contents

List of Figures

List of Tables

Chapter 1. Introduction

1.1 Background

Whitetopping is a pavement system of Portland cement concrete (PCC) placed on hot mix asphalt concrete (HMAC) pavement. Whitetopping is used to address distresses in asphalt pavement such as rutting and shoving. Three types of whitetopping pavements are commonly used. These types are classified according to the PCC slab thickness as follows:

- ultra-thin whitetopping (UTW): slab thickness between two to less than four inches
- thin whitetopping (TWT): slab thickness of four to less than eight inches
- conventional white topping: slab thickness of eight inches or more.

Whether whitetopping is a good candidate for the rehabilitation of deteriorated HMAC pavement depends on the supporting capability of the existing HMAC pavement. Without proper evaluations of the existing HMAC pavement, it is quite difficult to arrive at reasonable and effective rehabilitation strategies. In current rigid pavement design philosophy, the support condition is considered to have minor effects on long-term performance. It is because the stress level on the top of the subbase is kept quite low due to the high stiffness of the concrete slab and relatively large thickness of concrete slabs used in modern PCC pavements. Even though the evaluations of PCC pavements in Texas do not necessarily agree with this philosophy, it is indeed true that the stress level on top of the subbase due to the applications of wheel loading is quite low. However, the same philosophy cannot be applied to the whitetopping system. First, the slab thickness for whitetopping is smaller than that used in normal PCC pavement. Second, the joint system used in whitetopping does not fully utilize the benefits of the bending action of the slabs. The resulting effects are that the stress level on top of the HMAC pavement is not as small as that on top of the subbase in traditional PCC pavement. Accordingly, the performance of the whitetopping system depends on two structural factors: the support condition provided by the existing HMAC pavement and the combination of proposed PCC slab thickness and joint layouts. The required thickness for a given traffic application highly depends on the support conditions of the existing HMAC pavement.

Some of the difficulties facing pavement engineers who are considering the use of PCC overlay on a HMAC pavement include (1) is the existing HMAC section in need of rehabilitation a good candidate for PCC overlay? and (2) if so, what should be the optimum PCC overlay structure, whitetopping or regular full depth PCC pavement?

Many states agencies including the Texas Department of Transportation (TxDOT) have used whitetopping overlays and reported positive results. Traffic interruptions at intersections and along main arterials due to frequent repair or rehabilitation activities are often associated with delay and high user cost. In such cases, it is desirable to build a durable and reliable pavement system that requires minimum repair and rehabilitation activities. If designed and constructed properly, whitetopping could meet these requirement and help in mitigating the adverse effects associated with frequent and costly pavement repairs and rehabilitations.

TxDOT developed design standards and special specifications for thin whitetopping. Currently, however, the agency does not have guidelines or design procedures for the rehabilitation of HMAC pavement exhibiting rutting and shoving. Proper design procedures and guidelines for the use of whitetopping will improve the efficiency of TxDOT's operations in rehabilitation of deteriorated HMAC pavements.

1.2 Objectives

The primary objective of this research undertaking is to develop guidelines and design procedures for whitetopping in consideration of life-cycle cost analysis for statewide implementation. It is anticipated that the products of this research project will enhance TxDOT engineers' ability to develop the most cost-effective rehabilitation strategies for distressed HMAC pavement.

1.3 Scope

This report presents the findings of the literature search on whitetopping. The literature search focused on two areas. One is the review of the performance of whitetopping projects in various parts of the country. Efforts were made to identify the common characteristics that contributed to the good performance of whitetopping. The other is the review of design procedures currently available. Chapter 2 discusses the findings of a detailed literature review of the performance of whitetopping projects in the United States. Chapter 3 reviews currently available design methodologies for whitetopping. Detailed discussions are provided regarding how the design procedures were developed. Chapter 4 summarizes the previous chapters and presents the conclusions and recommendations.

Chapter 2. In-Depth Literature Review on Whitetopping Performance

2.1 Illinois

Illinois DOT (2002) constructed seven experimental whitetopping projects between 1998 and 2001. The performance of these projects was monitored through visual distress surveys and data collected on cracking, areas of debonding, and panel movements. Table 2.1 gives a description for each sub-project.

Table 2.1: Information Pertaining to Illinois DOT (2002) Projects

Project No.	Location	Route No.	Length	Construction Date	Overlay Thickness	Overlaid Surface
1	Decatur	U.S. 36	Intersection	April 1998	3.5 in.	1/3 PCC 2/3 Bit. Conc.
2	Decatur	U.S. 36	Intersection	April–May 1998	3.5 in. EB 2.5 in. WB	PCC
3	Carbondale	U.S. 51	Intersection	June–July 1998	3.5 in.	1/2 PCC 1/2 Bit. Conc.
4	Tuscola	U.S. 36	0.8 miles	May 1999	4–7.5 in.	Bit. Conc.
5	Clay County	CH3	7.85 miles	August 1998	5 in. and 6 in.	Bit. Conc.
6	Piatt County	CH4	4.94 miles	Sep.–Oct. 2000	5 in.	Bit. Conc.
7	Cumberland County	CH2	3.54 miles	September 2001	5.75 in.	Bit. Conc.

Project 1 was constructed in April 1998 with an average panel dimension of 3.6 feet by 4.3 feet. Three annual surveys were completed on this project. The number of panels was 181, four of which experience cracks in the first year. Fourteen panels were cracked in the second year and 21 panels showed crakes in the third year after construction. The most common cracking pattern was a transverse, mid-panel crack with a few corner breaks and random cracks. The panels within the driving lane appear to be shifting toward the intersection in relation to the outside row of panels. The movement was approximately 2 inches. Figure 2.1 shows the panel movement. The panel movement indicates poor or no aggregate interlock.

Figure 2.1: Panel Movements in Project 1

Project 2 included a thin bonded concrete overlay over concrete, not whitetopping.

Project 3 was constructed during June and July 1998. The average panel dimension was 3.2 feet by 3.3 feet. Polypropolene fibers were incorporated at the rate of three pounds per cubic yard into the concrete mixture to reduce early plastic shrinkage cracks. Three annual surveys were completed on this project. This project included 906 panels. The number of cracked panels was four (0.4%) for the first year, seven (0.8%) for the second year, and nine (1.0%) for the third year after construction.

Project 4 included conventional whitetopping sections. It was completed in May 1999. The project consists of conventional whitetopping with an overlay thickness ranging from 4 to 7 inches. Typical panel dimensions for this project were 5.0 feet by 5.5 feet. Two annual surveys on the project were completed. These surveys included 4809 panels. The number of cracked panels was 51 (1.1%) for the first year, and 96 (2.0%) for the second year after construction. Two of the 96 total cracks were surveyed in 2001 as transverse, mid-panel cracks. The remaining 94 cracks were all corner breaks similar to that shown in Figure 2.2. All cracks were of low severity, and no evidence of debonding was detected at this time.

Figure 2.2: Panel Corner Break for Project 4

Project 5 is a conventional whitetopping section that was completed during August 1998. The entire length of this project consisted of a conventional whitetopping with an overlay thicknesses of 5 to 6 inches. These sections were sawn at a 10 to 15 degree skewed angle. Three annual surveys were completed for this test section. Cracks and distresses were not detected on this section.

Project 6 included conventional whitetopping sections with an overlay thickness of 5 inches. It was completed in October 2000. Due to the length of this project, one experimental test section and one control section were selected for evaluation. One annual survey was completed on each section. The experimental section included all of the panels with 5.5 foot skewed transverse joints and 5.5 foot longitudinal joints. This section is approximately 2,630 feet long. The control section includes 100 panels with 11 foot skewed transverse joints. This section is approximately 550 feet long. Nine cracks were found in the experimental section, all of which were corner breaks. The corner breaks occurred at the corner of the panel where the skewed transverse joint formed an acute angle with the edge of the pavement. The cracks were all rated as low severity cracks. No cracks were found in the control section.

Project 7 section was completed in September 2001. This entire project is a conventional whitetopping with an overlay thickness of 5.75 inches. Transverse joints were sawn at intervals of 5.5 feet and longitudinal joints sawn at intervals of 6.0 feet. The transverse saw joints were skewed at an angle of 10 to 15 degrees. A six-month survey was completed in May 2002. Each experimental test section contains 120 rows of panels (480 total panels), and is approximately 660 feet long. Four panels had low severity transverse cracks.

Table 2.2 gives information on the pertinent construction costs for all of the whitetopping projects. Smaller panel sizes will increase the overall cost of the project due to the increased saw cutting cost.

Table 2.2: Project Construction Cost Information

Construction Item	Cumberland County – County Highway 2 (2001)	Piatt County – County Highway 4 (2000)	Clay County – County Highway 3 (1998)	Tuscola – U. S. Highway 36 (1999)	Carbondale – U. S. Highway 51 & Pleasant Hill Road (1998)	Decatur – U. S. Highway 36 & Country Club Road (1998)	Decatur – U. S. Highway 36 & Oakland Avenue
Pavement Milling 1.5 inches (sq. yds.)			$0.17 (102,283)				
Pavement Milling 3.0 inches (sq. yds.)	$1.11 (50,207)	$1.61 (63,490)					
Pavement Milling 3.5 inches (sq. yds.)					$6.86 (2,147)	$7.23 (2,563)	$7.23 (537)
Concrete Placement 2.5 inches (sq. yds.)						$18.72 (1,216)	
Concrete Placement 3.5 inches (sq. yds.)					$24.87 (2,147)	$21.20 (1,347)	$21.20 (537)
Concrete Placement 5.0 inches (sq. yds.)		$13.85 (63,490)	$12.56 (94,502)				
Concrete Placement 5.75 inches (sq. yds.)	$15.84 (50,207)						
Concrete Placement 6.0 inches (sq. yds.)			$13.89 (6,478)				
Concrete Placement Various (sq. yds.)				$17.69 (10,526)			
Saw Joints Partial-Depth (feet)	*	*	*	$0.72 (36,394)			
Saw Joints Full-Depth (feet)	*	*	*	$2.65 (7,710)			
Saw Joints Combined (feet)					$1.83 (9,921)	$1.15 (9,200)	$1.15 (2,267)
Total Cost (Per Square Yard)	$16.95	$15.46	$12.73 (5") $14.06 (6")	$22.08	$40.19	$30.08 (2.5") $32.56 (3.5")	$33.28

* Indicates this item was included with the cost of concrete placement.

2.1.1 Summary

The initial performance data of the seven projects above show that ultra-thin whitetopping may manifest panel movement. This panel movement indicates poor or no aggregate interlock. Ninety-four out of the 96 cracks found in Project 4 were all corner breaks. Most of the distresses in the whitetopping were mid-panel cracks or corner cracks. Overall early performance of whitetopping in project 1 was satisfactory. From the given information, smaller panel sizes will increase the overall cost of the project due to the increased saw cutting cost.

2.2 Minnesota

Three ultra-thin whitetopping (UTW) and three thin whitetopping pavement test sections were constructed, and extensive field testing was conducted at the Minnesota Road Research System (MnROAD) in 1997. Field performance data was provided. The ultra-thin whitetopping test

sections were designated as test cells 93, 94, and 95. Three whitetopping test cells were also constructed, but will not be considered in this study.

Table 2.3 describes slab thickness, panel size, and fiber type of the UTW test cells. Traffic loading of test cells 93, 94, and 95 consisted of approximately 26,400 annual average daily traffic (AADT), with 14% heavy commercial annual average daily traffic (HCAADT). These test cells were constructed in 1997 and had carried approximately 6 million rigid equivalent single axle loads (ESALs) in the right driving lane, in addition to 1.5 million CESALs in the passing lane as of June 2004. This report presents the performance history for the UTW test cells.

Figures 2.3 through 2.5 show the ride quality history for test cells 93, 94, and 95 respectively. Indices used in the ride quality are present serviceability rating (PSR) and the International Roughness Index (IRI), in m/km. The PSR is a subjective "seat of the pants" measure of pavement roughness determined by a group of people riding in similar vehicles. The IRI is a measure of the cumulative rise and fall of the pavement surface. It is determined using a laser device mounted on a special testing vehicle. The PSR is calculated from the IRI rating by Equation 2-1.

$$PSR = 6.634 - (2.813)\sqrt{IRI} \qquad \textbf{Eq. (2-1)}$$

The PSR has a scale of 0 (poor) to 5 (excellent), and a pavement is declared to have terminal serviceability when it declines to a value of 2.5 and below. As shown in Figures 2.3 through 2.5, the driving lane had reached values far below 2.5 in the spring of 2004. The cause of the low PSR was due to the distressed UTW surface. Figure 2.6 shows that cell 94, in particular, was experiencing punchout type distress in the corners of the interior panels near the wheelpaths. It is interesting to note the difference in performance between the driving and passing lanes in the UTW test cells.

The performance of UTW is clearly related to the volume of traffic loading. Other factors affecting the performance of UTW include the degree of bonding, the presence of moisture, and the geometry of the panels in relation to traffic loading. The types and quantities of cracking distress are summarized in Table 2.3.

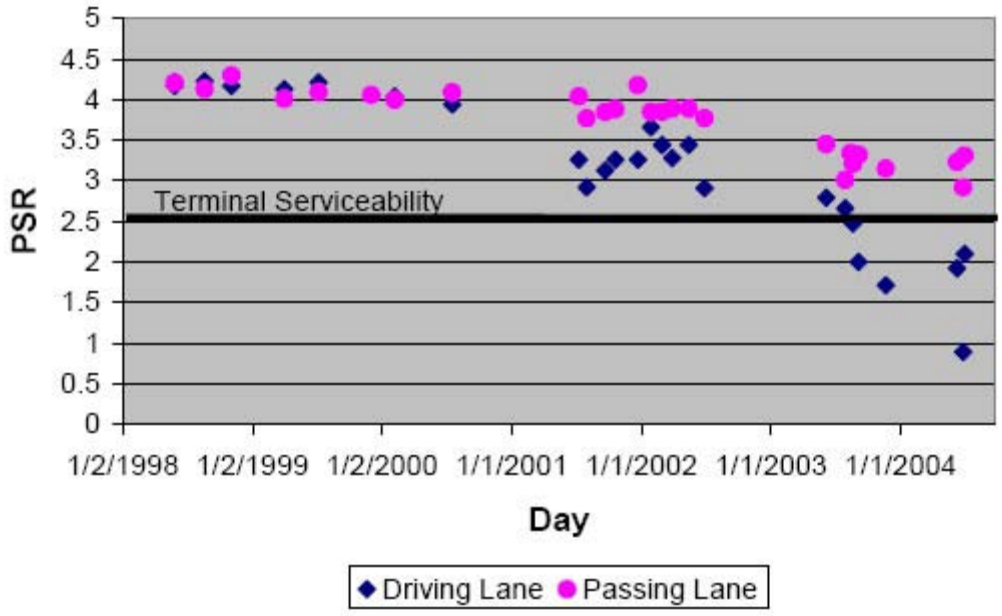

Figure 2.3: Ride Quality History for Test Cell 93

Table 2.3: Ultra-thin Whitetopping test cell design features

Test Cell Number	Concrete Slab Thickness, inches(mm)	Panel size feet (m)	Fiber Type
93 94 95	4 (102) 3 (76) 3 (76)	4×4 (1.2×1.2) 4×4 (1.2×1.2) 5×6 (1.5×1.8)	Polypropylene Polypropylene Polyolefin

Table 2.4: Type and quantities of distress for UTW test cells.

Test Cell	Corner cracks		Transverse cracks		Panels cracked (%) Panels repaired in 2001 not included	
	Driving Lane	Passing Lane	Driving Lane	Passing Lane	Driving Lane	Passing Lane
93	43	6	9	4	23	4
94	391	84	8	8	94	34
95	30	16	5	2	32	16

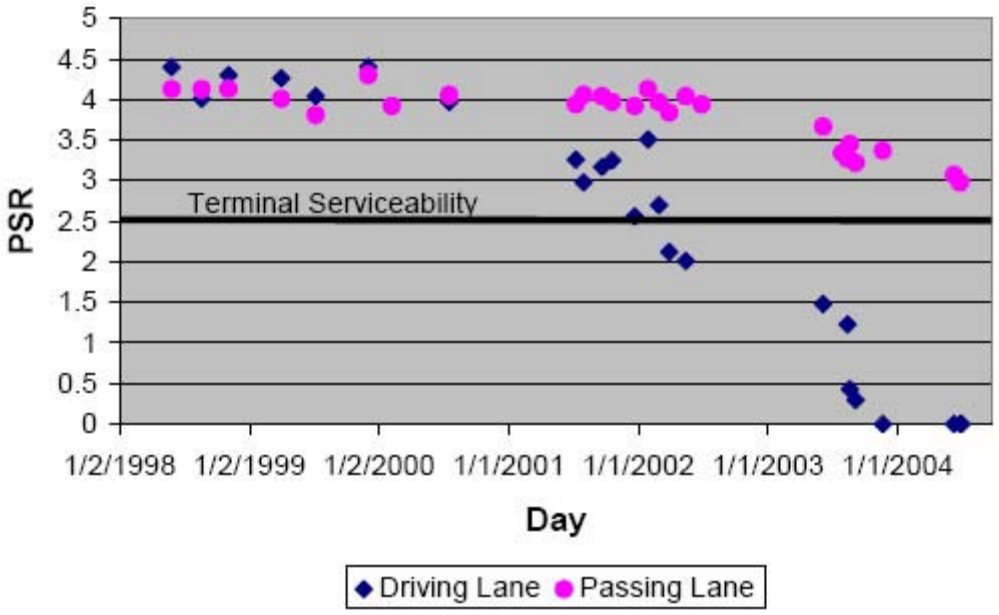

Figure 2.4: Ride Quality History for Test Cell 94

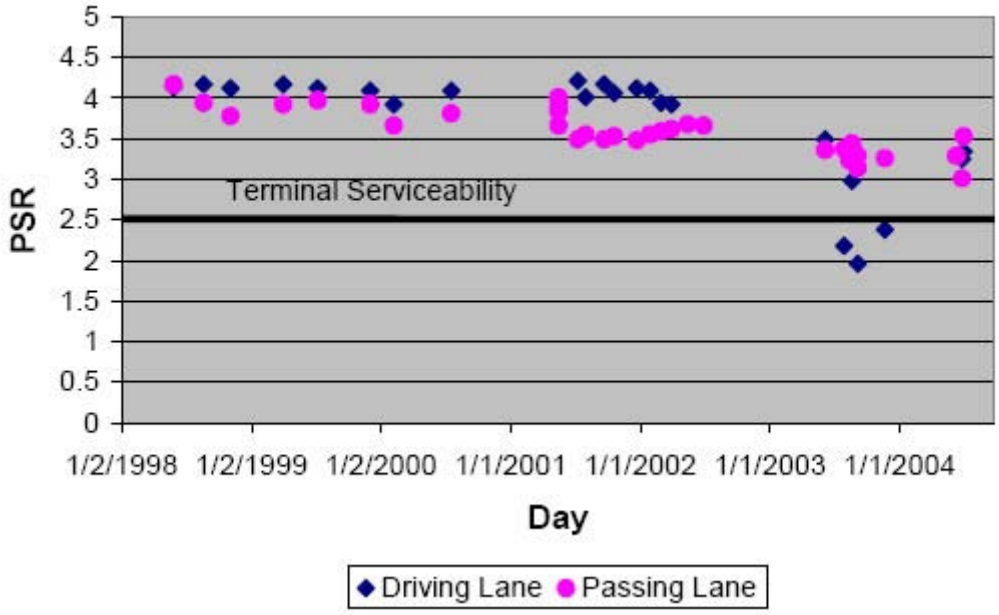

Figure 2.5: Ride Quality History for Test Cell 95

Figure 2.6: Corner cracked areas beginning to punch out in test cell 94

Test cell 93 consisted of a 4-inch thick UTW over 9 inches of hot-mix asphalt. This test cell experienced most surface distress in the form of corner cracking on the inside edge of the outer panels in the driving lane. Cracking was predominantly located on the approach side of the panels, nearest to the outside wheelpath of the driving lane. Figures 2.7 and 2.8 show examples of the distress before and after patching done by the Minnesota Department of Transportation (MnDOT) maintenance crews. The other predominant distresses in test cell 93 were reflective cracking (due to the bond with the HMA) and load related cracking. All but a few of these distresses were located in the outer panels of the driving lane, nearest to the shoulder (Figures 2.9 through 2.11).

Figure 2.7: Corner cracks near outside wheelpath in test cell 93

Figure 2.8: Patched corner crack areas near outside wheelpath of test cell 93 driving lane

Figure 2.9: Cracks from underlying asphalt layer reflected through UTW overlay in test cell 93

Figure 2.10: Load related cracking and surface depression (punchout) near existing transverse crack of test cell 93

Figure 2.11: Load related cracking and large surface depression of test cell 93 driving lane

Test cell 94 consists of a 3-inch thick UTW over 10 inches of hot-mix asphalt. This test cell experienced most surface distress in the form of corner cracking near the longitudinal joints of the center panels in the driving lane. Corner cracking was very extensive leading to center panels having diamond shaped punchouts near the corners. In some cases, the corner cracks were connected to each other (Figure 2.12). Figure 2.13 shows how extensive the corner crack patching was in the summer of 2004. The thinner panels of test cell 94 demonstrated more load related transverse cracking than test cell 93. By November 2003, the inside wheelpath of the passing lane in test cell 94 was starting to exhibit similar distress as the driving lane. As shown in Figure 2.14, the ride quality of the driving lane became so low (PSR=0) that interstate traffic was removed (for safety reasons) from the MnROAD mainline test sections on June 14, 2004.

Figure 2.12: Extensive corner cracking of test cell 94, November 2003.

Figure 2.13: Asphalt patching on nearly every panel in the driving lane of test cell 94, September 2004.

Figure 2.14: Passing lane of test cell 94, November 2003.

Similar to test cell 94, test cell 95 consists of a 3-inch thick UTW over 10 inches of hot-mix asphalt. However, this test cell experienced much less surface distress than test cell 94. The major difference is attributed to the larger panel size in test cell 95. Moving the wheelpath away from the longitudinal edges allows the thin 3-inch section to handle loads more efficiently. According to common theory in whitetopping design, if panel sizes are small, curling stresses will be reduced and the panels will deflect uniformly downward under the load. The performance of test cells 93 and 94 clearly demonstrate that a panel size of 4 by 4 feet is not a good design for high-volume traffic applications. Test cell 95 exhibited a fair amount of corner cracking on panel corners nearest the shoulder. This was true for both the driving and passing lanes. As shown in Figure 2.15 and 2.16, the corner cracking is always initiated on the approach side of the panel. Test cell 95 also had a small number of reflective cracks that grew large enough to warrant patching.

Figure 2.15: Corner cracking on the outside edge of test cell 95, for driving lane, November 2003

Figure 2.16: Corner cracking on the outside edge of test cell 95, for passing lane, November 2003

2.2.1 Summary

The performance history of different UTW test cells at MnROAD shows some variation in distress type and distress level. Test cells 93 and 94 developed severe corner cracking under the wheelpaths on the driving lane. Test cell 95 developed most cracking in the panels on the driving lane near the shoulder. Reflective and load related cracking were common on all test cells. All three test cells provided over 5 years of serviceability before reconstruction.

Findings related to performance analysis for MnDOT test cells show that joint spacing has a significant effect on performance. Additionally, corner cracking appears to be the primary failure mode, and fatigue cracking is believed to be the primary failure mechanism. Analysis also shows that bonding is an important factor to long-term performance. Ultra whitetopping provides small joint spacing to minimize restraint stress. However, joint locations and traffic loading should be given significant consideration. In the stress-reduction mechanism by bonding, debonding between layers always occurred near panel edges or cracks. The bond between layers was found to be intact near the center of panels.

2.3 Colorado

Four thin whitetopping test sections were constructed between 1996 and 2001 in Colorado. The first two were constructed on US 85 and SH119 in 1996. The third was constructed on US 287 in 1997 and the fourth section was constructed on SH 121 in 2001. Many variables were considered in the Colorado DOT test sections. These variables include concrete thickness, slab size, asphalt thickness, asphalt surface preparation, and the use of dowel and tie bars. Each site had multiple test sections and test slabs. Field testing was conducted at four different sites between 1996 and 2003. The tests were carried out to verify and revise design guidelines for bonded whitetopping pavement systems. The evaluation of the existing asphalt pavement condition prior to the thin whitetopping construction was performed including a visual condition survey, rutting measurements, coring, and falling weight deflectometer (FWD) testing.

Table 2.5 presents a summary of the test sections and certain section characteristics. Approximate traffic levels of AADT (Annual Average Daily Traffic) were estimated for each test section. The AADT levels included 1,500 (25% truck), 19,760 (8% truck), 2,287 (59% truck), and 44,562(3% truck) for US 85, SH 119, US 287, and SH 121, respectively.

Table 2.5: Test Slab Characteristics and Test Results

Site	Test Slab	PCC Thickness, in.	AC Thickness, in.	Longitudinal Joint Spacing, in.	Transverse Joint Spacing, in.	AC Resilient Modulus, psi	AC Surface Condition	Modulus of Subgrade Reaction, psi/in.
U.S. 85 Santa Fe	1	4.7	4.5	60	60	350,000	New	150
	2	5.8	5.9	60	60	350,000	New	150
	3	6.0	5.4	60	60	350,000	New Milled	150
S.H. 119 Longmont	1	5.1	3.3	72	72	800,000	Existing	340
	2	5.4	4.6	120	144	800,000	New	340
	3	6.3	3.4	72	72	800,000	New	340
	4	7.3	3.4	72	144	800,000	Existing Milled	340
	5	6.8	2.8	144	144	800,000	Existing Milled	340
U.S. 287 Lamar	B	7.4	7.0	144	120	800,000	Existing Milled	225
	E	6.8	6.6	72	72	800,000	Existing Milled	225
	F	5.6	6.6	72	72	800,000	Existing Milled	225
S.H. 121 Wadsworth	1	4.1	5.3	48	48	398,000	Existing Milled	500
	2	4.4	5.5	72	72	288,000	Existing Milled	500
	3	7.0	4.6	72	108	334,000	Existing Milled	500
	4	6.3	5.0	72	72	394,000	Existing Milled	500

Three test sections, out of four, were considered to examine the overall pavement performance during June 2003, after seven years of service. The task included crack mapping, core sampling, faulting measurements, joint width measurements, photographs, and FWD testing.

The overall condition of the US 85 test section was very good. Isolated longitudinal cracks were observed and a few corner cracks and transverse shrinkage cracks appeared to be located over longitudinal joint tie bars. Figures 2.17 and 2.18 present typical pavement conditions and a distressed area for the US 85 test section.

Figure 2.17: Typical Pavement Condition

Figure 2.18: Distressed Area at Stop Sign Approach (we need better title)

One hundred and thirty-one panels were surveyed on the SH 119 test section, 107 of which suffered some cracking. Figure 2.20 shows some severe full panel length cracks. These cracks were filled with asphalt sealant. In addition to the longitudinal panel cracks in Section No.2 of the SH 119 test section, the most frequent distress observed was minor joint spalling at various locations along the test sections. However, the overall ride quality was qualitatively rated as

excellent and the overall pavement condition was very good. Figures 2.19 and 2.20 present typical pavement condition including slab cracking in section No.2. A summary of the distress observed at the sites is presented in Table 2.6.

Figure 2.19: Typical Pavement Condition

Figure 2.20: Slab Cracking Filled with Asphalt Sealant

Table 2.6: Summary of Distress

SITE	SECTION	NUMBER OF SLABS SURVEYED	NUMBER OF CRACKED SLABS	QUANTITY OF CRACKS				
				Transverse Mid Panel	Corner	Longitudial Wheelpath	Longitudinal Mid-Panel	Other
U.S. 65 Frontage Road	Strain Test Slab No. 1	45	8	****	4	****	****	2
	Strain Test Slab No. 2	45	0	****	****	****	****	****
	Strain Test Slab No. 3	45	0	****	****	****	****	****
	Remainder of Pavement Section	369	94	2	35	2	12	26 39 2
U.S. 287	Test Section B	64	5	****	****	2	****	5
	Test Section F	200	33	2	2	20	4	9 5 4 11
	Test Section E	200	8	1	****	4	****	3 4 2
S.H. 119	Test Section No. 1	200	0	****	****	****	****	****
	Test Section No. 2	131	107	****	2	3	94	2
	Test Section No. 3	286	0	****	****	****	****	****
	Test Section No. 4	229	4	****	3	****	2	****
	Test Section No. 5	50	0	****	****	****	****	****

The most frequent distress observed in the US 287 test section was minor transverse joint spalling. In addition, isolated longitudinal cracking was observed in one of the 6 by 6 foot slab test sections. Approximately, 33 of the 200 slabs surveyed were cracked. Many of the cracks observed in this section appeared to be located in the outside wheel path. The overall ride quality was qualitatively rated as excellent, and the overall condition was also very good. Figures 2.21 and 2.22 show typical pavement conditions and cracked slabs.

Figure 2.21: Typical Pavement Condition

Figure 2.22: Cracked Slabs

2.3.1 Summary

Based on the study findings, partially bonded systems should be considered in the whitetopping design procedure. A good bond between concrete and asphalt is essential for successful whitetopping performance. It is recommended that joint spacing for thin whitetopping pavements

be 6 feet in both directions. At joint spacings greater than 4 feet, the temperature gradient in the concrete layer increases the load-induced tensile stress. Dowel bars at transverse contraction joints are not critical to attain satisfactory thin whitetopping pavement performance based on the performance of existing Colorado thin whitetopping test sections. Long-term monitoring is needed to determine the effect of load transfer devices.

Chapter 3. In-Depth Literature Review on Design Procedures

3.1 Colorado Design Procedure

Colorado design procedures for Whitetopping and Thin Whitetopping were published in 1998 and 2004. The reports describe a slightly thicker slab (4 to 8 inch) and wider joint spacing (up to 12 feet) than thin whitetopping. The reports suggest a guideline for the thickness design of bonded whitetopping pavement in the state of Colorado. In this report, the Colorado Department of Transportation (CDOT) performed laboratory testing and field testing at three different sites. The objectives of the field testing were to identify the critical load location, the effects of AC surface preparation, the response of whitetopping pavements to traffic loading, the interface bonding strength, the effect of pavement age on load-induced stresses, and the calibration of design guidelines developed. Laboratory tests were conducted on compressive strength, modulus of elasticity, and flexural strength after casting concrete cylinders and beams at test sites. Cores were used to measured thickness. Direct shear testing was performed to determine the interface shear strength between the concrete and asphalt layers.

3.1.1 Determination of Critical Load Location

The critical load location was determined by comparing the stress data collected for each load position. The highest tensile stress was determined when the load was centered along a longitudinal free-edge joint. Figure 3.1 shows the location of load resulting in maximum stress. Equation 3.1 was used in the design procedure.

$$\sigma_{FE} = 1.87 \times \sigma_{TE} \qquad \textbf{Eq. (3.1)}$$

Where: σ_{FE} is the free edge stress, and
σ_{TE} is the tied edge stress

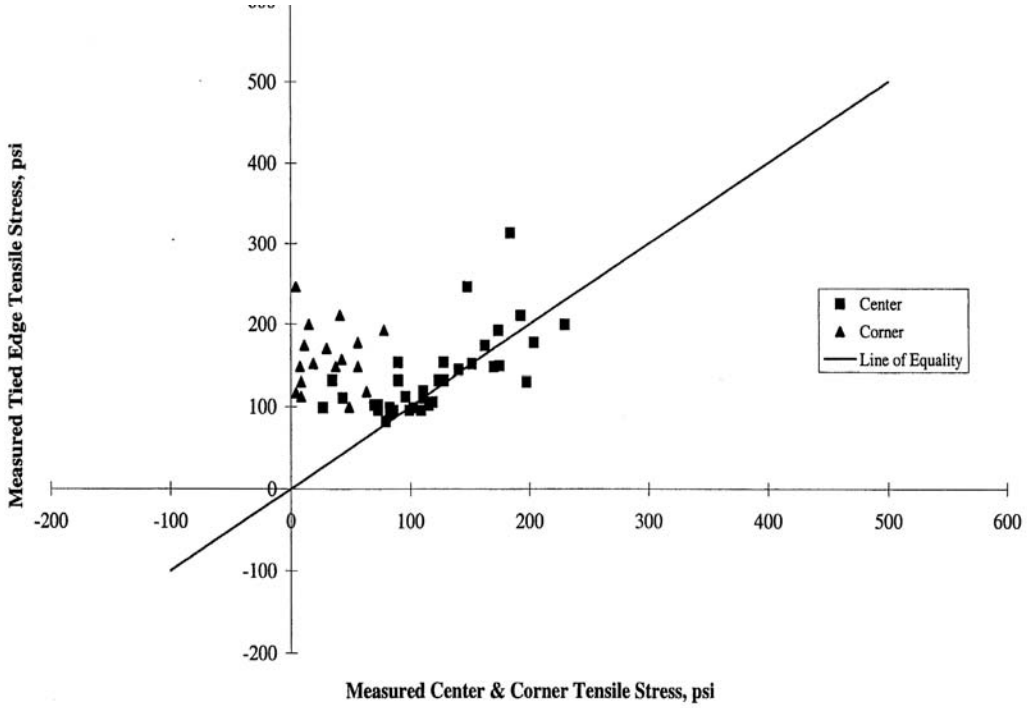

Figure 3.1: Location of Load Resulting in Maximum Stress

3.1.2 Determination of Load-Induced Stress at Zero Temperature Gradient

Zero temperature gradient stresses were compared with theoretically derived stresses. This comparison was to allow for a partial bond calibration factor to be applied to fully bonded theoretical stresses.

Analysis of the Effect of Bond Interface on Load-Induced Concrete Stress

Stresses caused by loads at mid-joint and slab corner were computed using the finite element computer program ILLISLAB (ILSL2), assuming fully bonded concrete-asphalt interface. Partial bond stresses were measured at tied edges. These stresses were greater than theoretically calculated stresses. Equations 3.2 and 3.3 represent the original and revised models respectively. Figure 3.2 show the calculated stresses using both the original and revised models.

1998 Original Model $\sigma_{ex} = 1.65 \times \sigma_{th}$ **Eq. (3.2)**

2004 Adjusted Model $\sigma_{ex} = 1.51 \times \sigma_{th}$ **Eq. (3.3)**

where: σ_{th} is the theoretical stress

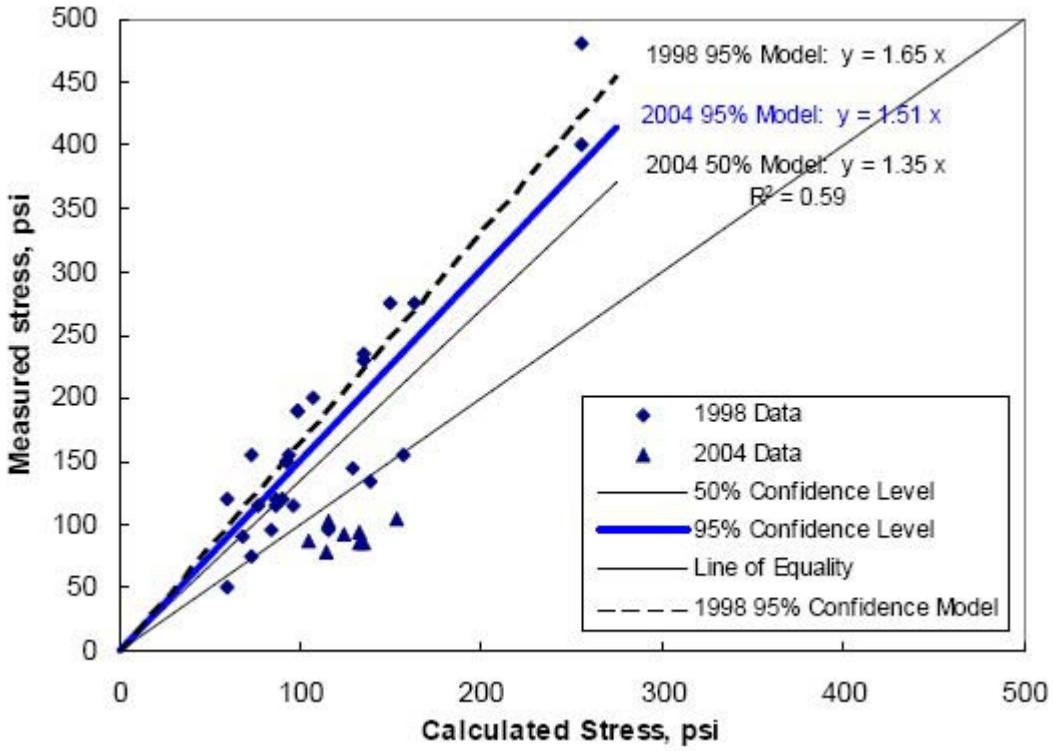

Figure 3.2: Increase in Critical Load Stress Due to Partial Bonding Condition

3.1.3 Analysis of the Effect of Interface Bond on Load-Induced Asphalt Strain

Prior to construction, strain gages were placed at the surface of the asphalt and the bottom of the concrete. There is approximately a 10 percent loss of strain transfer from the concrete to the asphalt due to the partial bond between the layers. This shows a decrease of 15 percent from the readings determined in the original study. Figure 3.3 shows a comparison of asphalt and concrete strains for the tied edge loading case. The equations representing the loss of strain are as follows:

1998 Original Model $\varepsilon_{ac} = 0.842 \times \varepsilon_{pcc}$ **Eq. (3.4)**

2004 Adjusted Model $\varepsilon_{ac} = 0.897 \times \varepsilon_{pcc} - 0.776$ **Eq. (3.5)**

where,

εac = measured asphalt surface strain, microstrain

εpcc = measured concrete bottom strain, microstrain

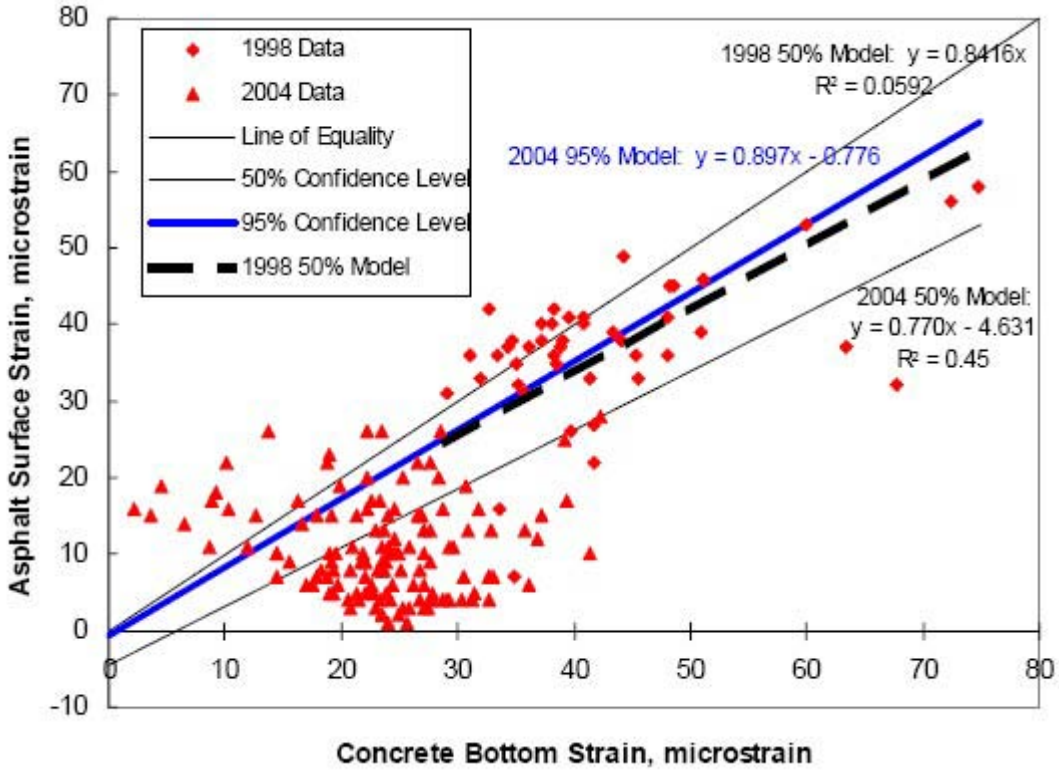

Figure 3.3: Asphalt Surface Strain vs. Concrete Bottom Strain

3.1.4 Analysis of Temperature Effects on Load-Induced Stresses

Temperature gradients throughout load testing ranged from -2 to 6°F/in. Figure 3.4 shows the percent change in measured stress over the range of temperature gradients tested. The relationships derived between the change in stress and measured temperature gradient is as follows:

1998 Original Model $\sigma_{\%} = 4.56 \times \Delta_T$ **Eq. (3.6)**

2004 Adjusted Model $\sigma_{\%} = 3.85 \times \Delta_T$ **Eq. (3.7)**

Where: $\sigma_{\%}$ is percent change in stress from zero gradient.

Δ_T is the change in temperature.

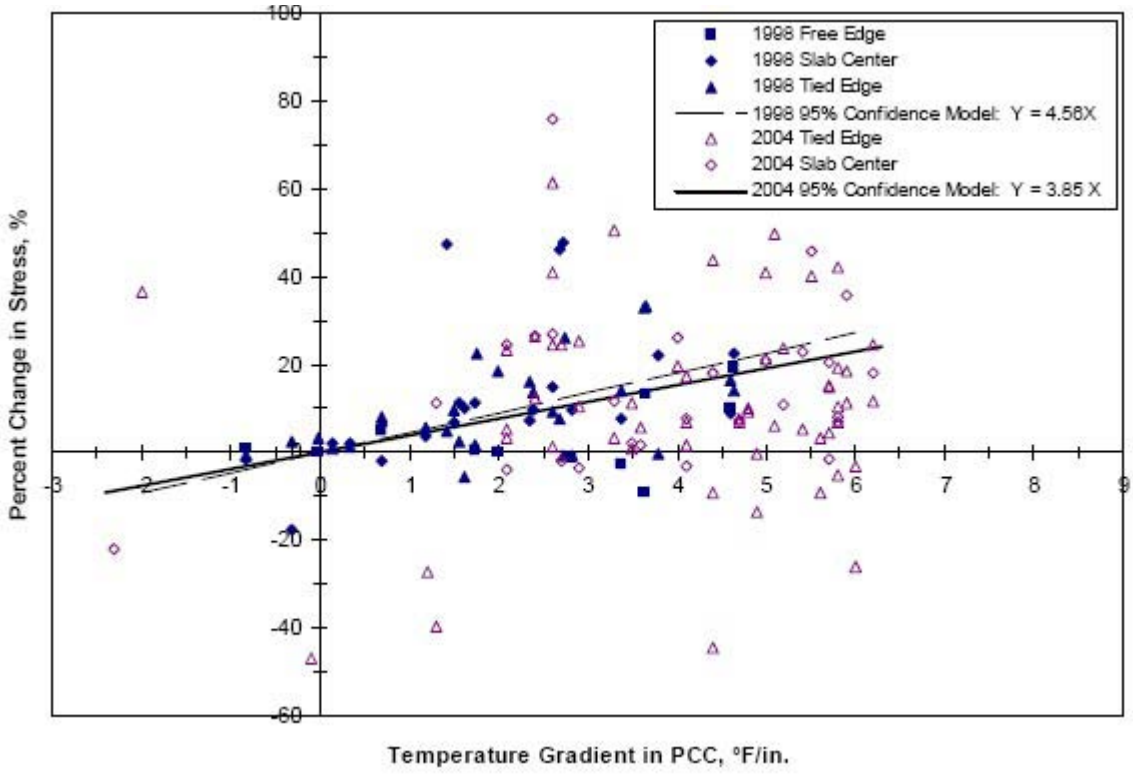

Figure 3.4: Increase in Load Stress Due to Curling Loss of Support

3.1.5 Development of Revised Design Equations

Stress calculations were conducted using the finite element program ILLISLAB (ILSL2). Curling and warping restraint stresses were not incorporated into the parametric analysis. Prediction equations were derived for computing design concrete flexural stresses and asphalt flexural strains. Table 3.1 lists the combinations of parameters. The derived equations and revised equations were as follows:

(1998 Original Prediction Equations for Design Stresses and Strains)

Concrete Stress for 20-kip single axle load (SAL)

$$\sigma_{pcc} = 919 + \frac{18492}{l_e} - 575.3 \log k + 0.000133 E_{ac} \qquad \textbf{Eq. (3.8)}$$

Concrete Stress for 40-kip tandem axle load (TAL)

$$\sigma_{pcc} = 671.2 - 0.000099 E_{ac} - 437.1 \log k + \frac{1.582 \times 10^4}{l_e} \qquad \textbf{Eq. (3.9)}$$

Asphalt Strain for 20-kip SAL

$$\frac{1}{\varepsilon_{ac}} = 8.51114 \times 10^{-9} E_{ac} + \frac{0.008619 l_e}{L} \qquad \textbf{Eq. (3.10)}$$

Asphalt Strain for 40-kip TAL

$$\frac{1}{\varepsilon_{ac}} = 9.61792\times10^{-9} E_{ac} + \frac{0.009776 l_e}{L} \qquad \textbf{Eq. (3.11)}$$

where,
σpcc = maximum stress in the concrete slab, psi
εac = maximum strains at bottom of asphalt layer, microstrain
Epcc = concrete modulus of elasticity, assumed 4 million psi
Eac = asphalt modulus of elasticity, psi
tpcc = thickness of the concrete layer, in.
tac = thickness of the asphalt layer, in.
μpcc = Poissons ratio for the concrete, assumed 0.15
μac = Poissons ratio for the asphalt, assumed 0.35
k = modulus of subgrade reaction, pci
le = effective radius of relative stiffness for fully bonded slabs, in.
= {Epcc * [tpcc
3 / 12 + tpcc * (NA - tpcc / 2)2] / [k * (1 - μpcc
2)]
+ Eac * [tac
3 / 12 + tac *(tpcc - NA + tac / 2)2] / [k * (1 - μac
2)]} ¼
NA = neutral axis from top of concrete slab, in.
= [Epcc * tpcc
2 / 2 + Eac * tac * (tpcc + tac / 2)] / [Epcc * tpcc + Eac * tac]
L = joint spacing, in.

2004 Revision of the Stresses and Strain Prediction Design Equations

Concrete Stress for 20-kip SAL

$$(\sigma_{pcc})^{1/2} = 18.879 + 2.918\frac{t_{pcc}}{t_{ac}} + \frac{425.44}{l_e} - 6.955\times10^{-6} E_{ac} - 9.0366\log k + 0.0133L$$

Eq. (3.12)

Concrete Stress for 40-kip TAL

$$(\sigma_{pcc})^{1/2} = 17.669 + 2.668\frac{t_{pcc}}{t_{ac}} + \frac{408.52}{l_e} - 6.455\times10^{-6} E_{ac} - 8.3576\log k + 0.00622L$$

Eq. (3.13)

Asphalt Strain for 20-kip SAL

$$(\varepsilon_{ac})^{1/4} = 8.224 - 0.2590\frac{t_{pcc}}{t_{ac}} - 0.04419 l_e - 6.898\times10^{-7} E_{ac} - 1.1027\log k$$

Eq. (3.14)

Asphalt Strain for 40-kip TAL

$$(\varepsilon_{ac})^{1/4} = 7.923 - 0.2503\frac{t_{pcc}}{t_{ac}} - 0.04331 l_e - 6.746\times10^{-7} E_{ac} - 1.0451\log k$$

Eq. (3.15)

where,
σpcc = maximum stress in the concrete slab, psi
εac = maximum strains at bottom of asphalt layer, microstrain
Epcc = concrete modulus of elasticity, assumed 4 million psi
Eac = asphalt modulus of elasticity, psi
tpcc = thickness of the concrete layer, in.
tac = thickness of the asphalt layer, in.
μpcc = Poissons ratio for the concrete, assumed 0.15
μac = Poissons ratio for the asphalt, assumed 0.35
k = modulus of subgrade reaction, pci
le = effective radius of relative stiffness for fully bonded slabs, in.
= {Epcc * [tpcc3 / 12 + tpcc * (NA - tpcc / 2)2] / [k * (1 - μpcc2)]+ Eac * [tac3 / 12 + tac *(tpcc - NA+ tac / 2)2] / [k * (1 - μac2)]} ¼
NA = neutral axis from top of concrete slab, in.= [Epcc * tpcc2 / 2 + Eac * tac * (tpcc + tac / 2)] / Epcc * tpcc + Eac * tac]
L = joint spacing, in.

Table 3.1: Combinations of Parameters

Parameters	Original 1998	Adjusted 2004
Joint spacing	48, 72, and 144in.	48, 72, and 144in.
Concrete slab thickness	4, 5, and 6in.	4, 5, 6, and 7in.
Asphalt thickness	3, 6, and 9in.	3, 6, and 9in.
Concrete modulus of elasticity	4million psi	4million psi
Asphalt modulus of elasticity	0.05, 0.5, and 1million psi	0.05, 0.25, 0.5, 0.75 and 1million psi
Concrete Poisson’s ratio	0.15	0.15
Asphalt Poisson’s ratio	0.35	0.35
Modulus of subgrade reaction	75, 200, and 400pci	50, 150, 300and 500pci
Truck axle configuration	Single(SAL) & Tandem(TAL)	Single(SAL) & Tandem(TAL)
Slab loading locations	Corner & Longitudinal Edge	Corner & Longitudinal Edge

3.1.6 Mechanistic Whitetopping Thickness Design Procedure

Design of whitetopping pavement should be determined considering material properties and design parameters. The design procedure is explained in 12-steps. Parameters required include percentage fatigue life of the existing asphalt pavement and assumed concrete slab thickness. Also, material properties needed are the existing modulus of subgrade reaction, temperature differential (temperature gradient; ℉/in.), joint spacing, modulus of elasticity, thickness, and

Poisson's ratio of asphalt and concrete, and modulus of rupture of concrete. A brief summary for thickness design procedures is give below.

(1) Design parameters, l_e and L/l_e are determined, then the load-induced critical concrete stresses and asphalt strains are calculated using developed equation for anticipated 20-kip single axle loads (SAL) and 40-kip tandem axle loads (TAL).

(2) Computed fully bonded concrete stresses and asphalt strains are adjusted using equations for the partial bond condition. The adjusted concrete stresses are computed for the loss of support due to temperature-induced concrete slab curling again.

(3) Fatigue analyses for concrete stresses and asphalt strains are conducted separately.

(4) Concrete thickness and joint spacing are determined so that they meet the fatigue failure criteria. If not, the previous steps are repeated until they satisfy fatigue failure criteria.

Figure 3.5 exhibits the flow chart of the concrete thickness design procedure developed in Colorado State.

3.1.7 Sensitivity Analysis

Sensitivity analyses conducted for asphalt thickness, modulus of subbase/subgrade reaction, asphalt modulus of elasticity, concrete flexural strength and the expected number of 18-kip equivalent single axle loads (ESALs).

The 1998 study was sensitive to the modulus of subbase/subgrade reaction, but the 2004 study are much less sensitive to subgrade modulus. The 1998 study appeared to be fairly sensitive at very low asphalt moduli (50,000 psi), and there appeared to be a minimum asphalt thickness of about 5 inches. However, the 2004 sensitivity analysis shows more consistency with the general relationship that is expected between concrete thickness and asphalt modulus.

The thickness is slightly sensitive to the flexural strength of concrete. The thickness, however, was not sensitive to anticipated concrete temperature gradients. Required concrete thicknesses based on the 1998 study were not sensitive to the number of ESALs above 1 million except under various levels of asphalt modulus of elasticity. The 2004 revised design procedure is more sensitive to traffic levels for each of the design variables.

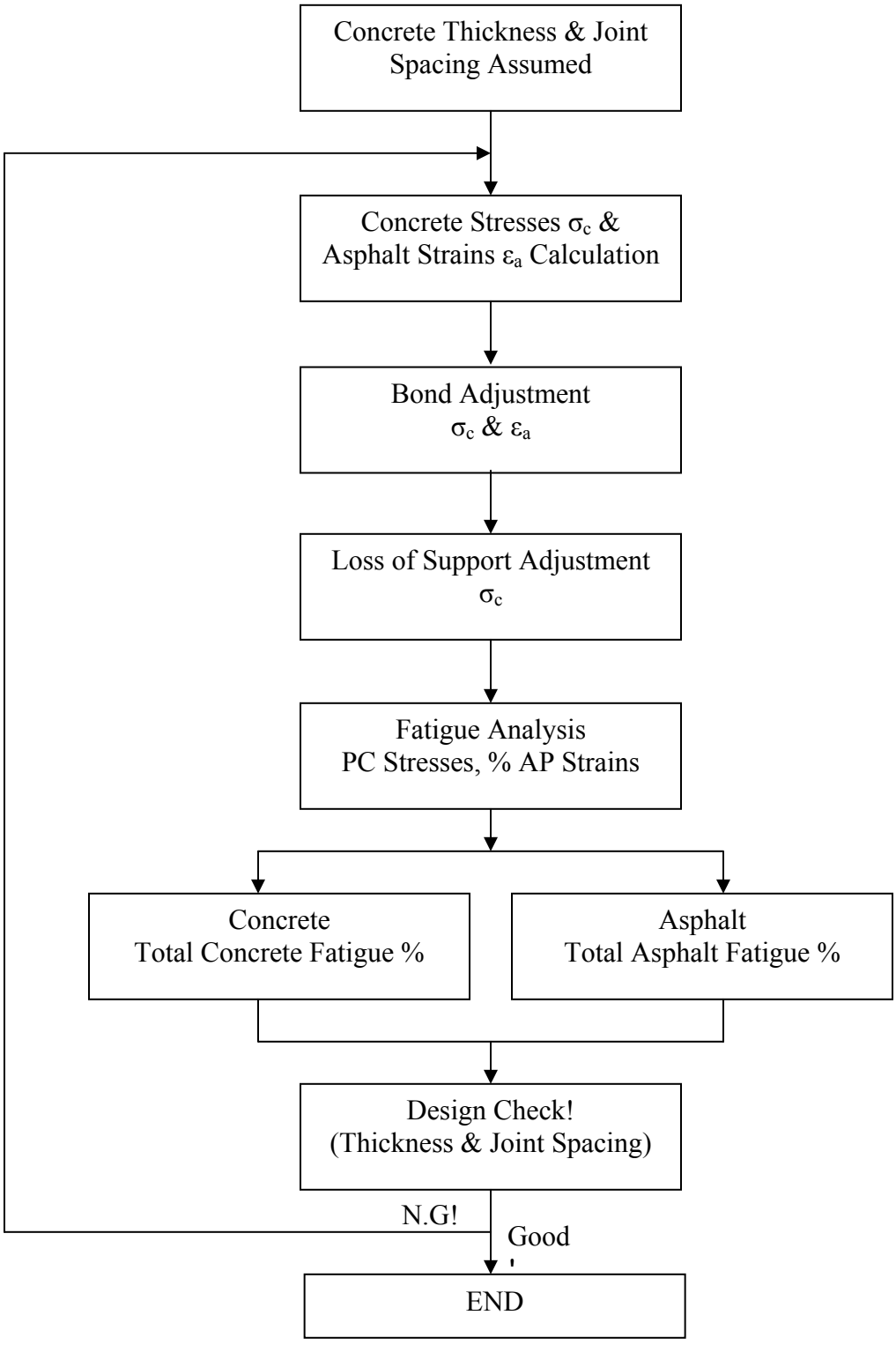

Figure 3.5: Flow Chart for Colorado Design Procedure

3.2 ACPA Design Procedure

The design and construction of conventional whitetopping and ultra-thin whitetopping are presented in this report. Four factors are considered in the structural design of concrete pavement: supporting strength of the existing asphalt pavement; flexural strength of the concrete; design period (the expected service life of the pavement before any major structural rehabilitation is required); and amount of truck traffic expected.

3.2.1 Support Provided by the Existing Asphalt Pavement

The support at the top of asphalt is determined by the k-value of the subgrade (k_s), the thickness of granular or cement-treated base, and the layer thickness of the existing asphalt. Figures 3.6 and 3.7 show the chart to estimate the k-value on top of the existing asphalt pavement according to base types.

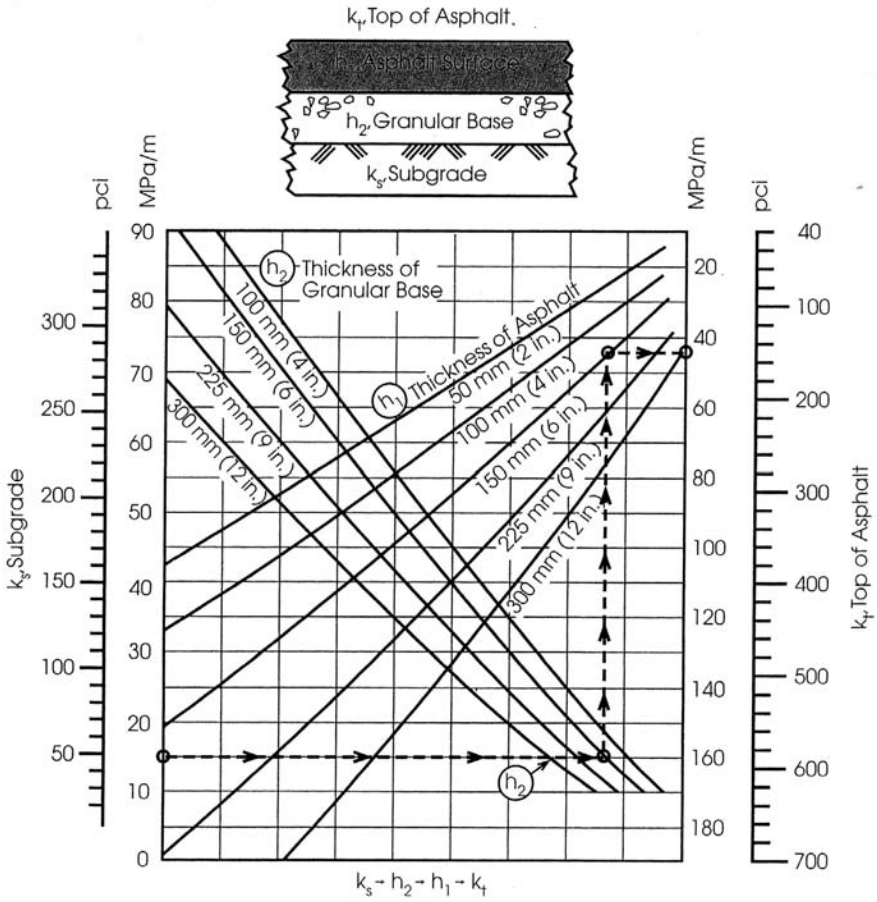

Figure 3.6: K-value on top of asphalt pavement with granular base

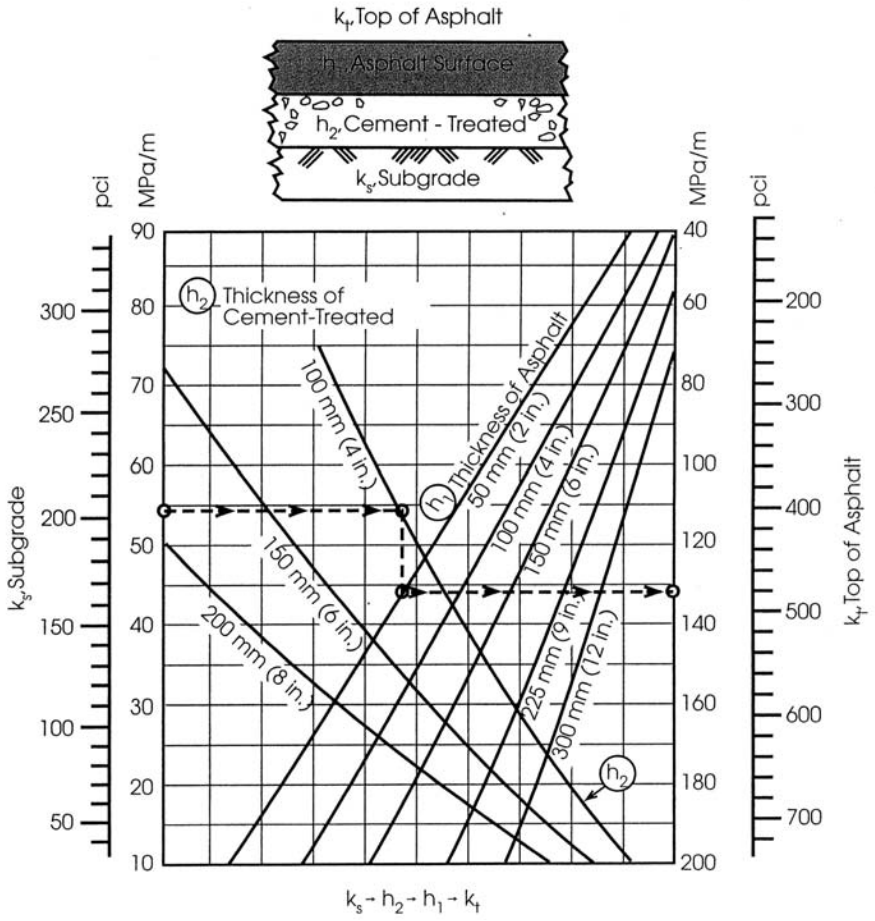

Figure 3.7: K-value on top of asphalt pavement with cement-treated base

The k-value of the subgrade (k_s) is usually determined by a plate load test, but can be calculated from falling-weight deflectometer (FWD). Also, approximate k-values for soil types are shown in Table 3.2.

Table 3.2: Subgrade Soil Types and Approximate k-value

Type of Soil	Support	k MPa/m (pci)	CBR	R
Fine-grained soils in which silt and clay-size particles predominate	Low	20-30 (75-120)	2.5-3.5	10-22
Sand and sand-gravel mixtures with moderate amounts of silt and clay	Medium	35-45 (130-170)	4.5-7.5	29-41
Sand and sand-gravel mixtures relatively free of plastic fines	High	50-60 (180-220)	8.5-12	45-52

CBR=California Bearing Ratio, ASTM D1183
R=Resistance R-Value, ASTM D2844

3.2.2 Flexural Strength Design Value for Concrete

Flexural strength design value for concrete pavement is considered to be the value measured at 28 days. However, if compressive strength of concrete is tested, the following equation, which is an approximate relationship between flexural and compressive strength may used.

$$f_r = C(f_{cr}')^{0.5} \qquad \textbf{Eq. (3.16)}$$

Where, f_r is flexural strength (modulus of rupture) MPa (psi), C is a constant, 0.75 metric (9 U.S.), and f_{cr} is compressive strength, MPa (psi).

Table 3.3 shows the relationship between compressive strength and flexural strength.

Table 3.3: Relationship between compressive strength and flexural strength

Metric		U.S.	
Compressive, MPa	Flexural, MPa	Compressive, psi	Flexural, psi
24	3.7	3500	530
28	4.0	4000	570
32	4.2	4500	600
36	4.5	5000	640

Note: For individual concretes, the constant, C may vary by ± 10 percent; concretes made with crushed aggregates usually have higher flexural strengths than those made with gravel or rounded aggregate.

3.2.3 Truck Traffic

Truck traffic considered in the design is the weight and number of daily repetitions. Other vehicles in the traffic stream are not considered. In the design table, the number of trucks, expressed as "trucks per day per lane" indicates how many load repetitions per day are applied on the pavement.

3.2.4 Design Period

Design period is generally considered as 20 years, it may be longer or shorter depending on the expected use of the facility. In this publication, design period of 20 years is considered.

3.2.5 Determination of Pavement Thickness

Slab thickness is determined by the amount of truck traffic, flexural strength of concrete, and support strength (k-value) on top of existing asphalt pavement. The ACPA design procedure is represented in Tables 3.4 and 3.5 for two traffic categories. One is for light to medium truck traffic. The other is for heavy truck traffic. The table shows that if the flexural strength of concrete and traffic are constant, then the slab thickness depends on the support reaction on top of existing asphalt pavement. Therefore, it is important to determine an accurate support reaction (k) of the existing asphalt pavement.

Table 3.4: Slab Thickness, Light to Medium Truck Traffic

Trucks per day per lane	Design flexural strength, psi (average)	k-value, pci									
		700		500		300		200		100	
2	650	4.5	(4.0)	4.5	(4.0)	5.0	(4.0)	5.5	(4.5)	6.0	(5.0)
	600	4.5	(4.0)	5.0	(4.0)	5.5	(4.5)	5.5	(4.5)	6.0	(5.0)
	550	5.0	(4.0)	5.5	(4.5)	5.5	(5.0)	6.0	(5.0)	6.5	(5.5)
10	650	4.5	(4.0)	5.0	(4.0)	5.5	(4.5)	5.5	(4.5)	6.0	(5.0)
	600	5.0	(4.0)	5.0	(4.5)	5.5	(4.5)	6.0	(5.0)	6.5	(5.5)
	550	5.5	(4.5)	5.5	(4.5)	6.0	(5.0)	6.5	(5.5)	7.0	(6.0)
40	650	5.0	(4.0)	5.0	(4.5)	5.5	(4.5)	6.0	(5.0)	6.5	(5.5)
	600	5.0	(4.5)	5.5	(4.5)	6.0	(5.0)	6.0	(5.5)	7.0	(6.0)
	550	5.5	(4.5)	6.0	(5.0)	6.5	(5.5)	6.5	(5.5)	7.0	(6.0)

Dowels are not required.
Parenthesis = pavement with edge support (concrete shoulder, widened lane, curb and gutter, or adjacent concrete lanes on both sides).
Minimum thickness = 4 in.

Table 3.5: Slab Thickness, Heavy Truck Traffic

Trucks per day per lane	Design flexural strength psi (average)	k-value, pci									
		700		500		300		200		100	
80	650	7.0	(6.0)	7.0	(6.0)	7.5	(6.5)	8.0	(7.0)	9.0	(7.5)
	600	7.0	(6.5)	7.5	(6.5)	8.0	(7.0)	8.5	(7.5)	9.5	(8.0)
	550	7.5	(6.5)	8.0	(7.0)	8.5	(7.5)	9.0	(8.0)	10.0	(8.5)
400	650	7.5	(7.0)	8.0	(7.0).	8.0	(7.5)	8.5	(7.5)	9.5	(8.0)
	600	7.5	(7.0)	8.0	(7.0)	8.5	(7.5)	9.0	(8.0)	10.0	(8.5)
	550	8.0	(7.0)	8.5	(7.5)	9.0	(8.0)	9.5	(8.5)	10.5	(9.0)
1200	650	7.5	(7.5)	8.0	(8.0)	8.5	(8.0)	9.0	(8.0)	9.5	(8.5)
	600	8.0	(7.5)	8.5	(8.0)	9.0	(8.5)	9.5	(8.0)	10.5	(9.0)
	550	8.5	(7.5)	9.0	(8.0)	9.5	(8.5)	10.0	(8.5)	11.0	(9.5)

Shaded = doweled joints, unshaded = undoweled joints.
Parenthesis = pavement with edge support (concrete shoulder, widened lane, curb and gutter, or adjacent concrete lanes on both sides).

3.3 New Jersey Design Procedure

The objective of this research study was to identify and address important factors that contribute to the performance of the UTW pavement system. The field testing of a UTW ramp that was constructed in New Jersey began in 1994. the testing was conducted using Heavy Weight Deflectometer (HWD), Falling Weight Deflectometer (FWD), and Dynamic Cone Penetrometer (DCP). In addition, a visual survey was conducted and pavement cores were tested. The performance of this UTW pavement was studied using a 3-Dimensional Finite Element Model (FEM). An interim design procedure was developed based on the experiences gained from field testing and the Finite Element Model.

3.3.1 Field Testing

Ultra-thin whitetopping pavement was constructed by New Jersey DOT (NJDOT) in August of 1994. Preparatory measures included milling the distressed bituminous surface. An average of three inches of milling was made prior to the placement of UTW. The panel sizes were 3 by 3 feet, 4 by 4 feet, and 6 by 6 feet.

Non-destructive testing using HWD and FWD was performed on a total of 45 locations—29 locations on 3-by-3 panels, 10 locations on 4-by-4 panels, and 6 locations on 6-by-6 panels. Deflection data was analyzed in order to determine the in-situ layer stiffnesses and load transfer capability of the saw cut joints. Dynamic Cone Penetrometer (DCP) testing was performed to obtain a continuous reading of California Bearing Ratio (CBR) with depth.

A visual survey was carried out in order to determine the areas of significant distress. The survey revealed that the major forms of visual distress for the pavement structure are cracking and corner breaking. ARAN equipment with automatic video was used to survey the pavement and measure its roughness. The data obtained was not available for review and may be used in conjunction with other findings in the field in the future.

A total of ten pavement cores were taken. The thickness of UTW and AC for each core was recorded. Three of the extracted cores were debonded at the interface. Other cores showed a strong bond at the interface but were broken in AC layer presumably due to coring operation. The average UTW thickness was 3.8 inches.

3.3.2 Finite Element Analysis and Verification

The modeling and analysis were performed by SAP2000 structural analysis program. Figures 3.8 to 3.9 show the finite element modeling. The model describes a four-layer pavement consisting of the UTW, AC base, granular subbase, and the subgrade. Parameters investigated and their ranges are shown in Table 3.6.

Table 3.6: Parameters Investigated

Parameters	Range
UTW thickness	3 to 5 inches
AC thickness	4 to 8 inches
AC modulus of elasticity	880 to 1660 ksi
Subbase modulus of elasticity	4.2 to 16.8 ksi
Modulus of subgrade reaction	145 to 580 pci
UTW slab size	3×3, 4×4
Interface bonding	from fully bonded to unbonded
Joint width and depth	0.5 inch and 1/3 of the thickness

The Westergaard equation is used to verify the finite element model. The maximum flexural stress in the slab can be approximately expressed as:

$$\sigma = \frac{0.316P}{h^2}\left[4\log\left(\frac{l}{b}\right)+1.069\right] \qquad \textbf{Eq. (3.17)}$$

Where P is the applied load, h is the slab thickness; b indicates the size of the resisting section of the slab; that is

$$b = \sqrt{1.6r^2 + h^2} - 0.675 \quad \text{if } r < 1.724h \qquad \textbf{Eq. (3.18)}$$

$$b = r \quad \text{if } r \geq 1.724h \qquad \textbf{Eq. (3.19)}$$

Finally, l is the radius of relative stiffness.

$$l = \sqrt[4]{\frac{Eh^3}{12(1-\mu^2)k}} \qquad \textbf{Eq. (3.20)}$$

Where, E and μ indicate the elastic modulus and Poisson's ratio of the slab respectively, and *k* represents the coefficient of subgrade reaction.

The results show that the maximum tensile stress for a 3-inch slab, modulus of 3400ksi, Poisson's ratio of 0.15, subgrade reaction of 250pci, and 12,000-pound load with 50psi air pressure, is equal to 758psi. The maximum tensile stress obtained from the finite element model is 785psi.

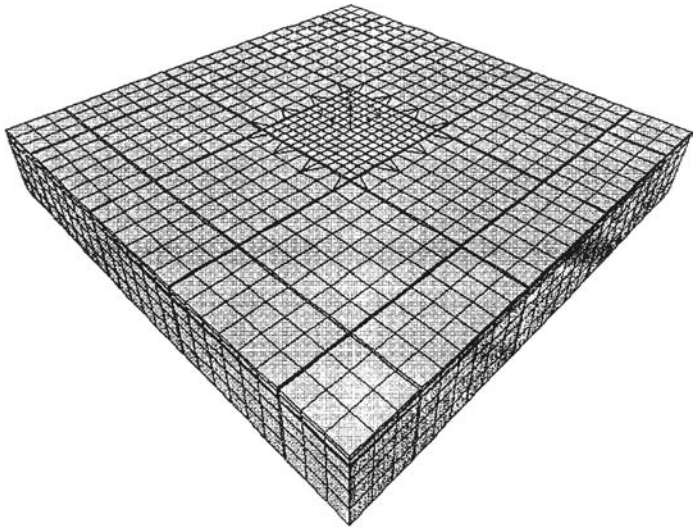

Figure 3.8: Finite Element Model

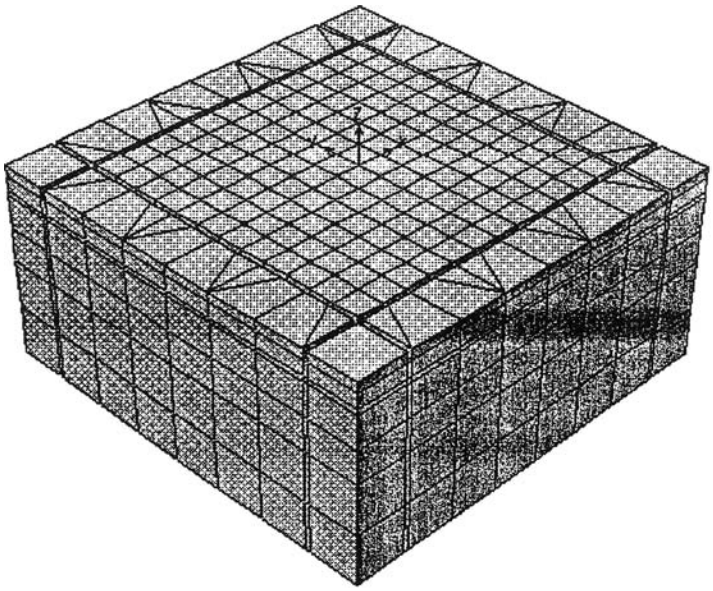

Figure 3.9: Detail of the finite element model

3.3.3 Design Procedure

The following steps are a summary for design procedure of UTW.

Step 1. Obtain the traffic data for the project and find the number of equivalent 18-kip single axle load. The traffic data, which is a combination of different vehicles, is converted to an equivalent 18-kip single axle to be used in fatigue equations. Equations 2.21-a, and 2.21-b are used for single axles and tandem axles, respectively.

$$W_{18} = \left(\frac{W_{SAL}}{18} \right)^{3.3} \qquad \textbf{Eq. (3.21-a),}$$

$$W_{18} = \left(\frac{TW_{TAL}}{2 \times 18} \right)^{3.3} \qquad \textbf{Eq. (3.21-b)}$$

It is recommended by AASHTO 1993 to use a safety factor by increasing the number of design ESAL based on the standard deviation of errors in traffic prediction and pavement performance in addition to the required design reliability.

$$W_D = 10^{-Z_R S_0} W_{18} \qquad \textbf{Eq. (3.22)}$$

Where, S_0 is the overall standard deviation of errors in design and Z_R is the standard normal deviate associated with design reliability.

Step 2. Obtain the elastic modulus and thickness of the existing asphalt pavement, as well as the coefficient of subgrade reaction using methods such as FWD.

Step 3. Calculate the allowable tensile stress in AC using the Fatigue equation developed by the Asphalt Institute and Portland Cement Association (Eq.3.23).

$$N = 0.058 \frac{E_a^{2.437}}{\sigma^{3.291}} \qquad \textbf{Eq. (3.23)}$$

Step 4. Assume a thickness for UTW and find the maximum tensile stress in AC using Equations 3.24 and 3.25 for both bonded and unbonded conditions. Equations to predict the design stresses in a UTW pavement system based on the finite element results of this study were developed. Based on the composite beam concept, the prediction equations for maximum tensile stress in AC with or without bond case were developed as follow

$$\sigma_B^{AC} = \frac{CP(N.A.-h)}{I_B}\left[C_1 \log(\frac{l}{b}) + C_2 \frac{N.A.}{a} + C_3\right] \qquad \textbf{Eq. (3.24)}$$

$$\sigma_U^{AC} = \frac{CPa}{2I_U}\left[C_1 \log(\frac{l}{b}) + C_2 \frac{a}{h} + C_3\right] \qquad \textbf{Eq. (3.25)}$$

Step 5. Compare the maximum tensile stress in AC against the allowable stress from Step 3.

Step 6. Repeat Steps 4 and 5 until the allowable stress and maximum tensile stress are equal.

Step 7. Calculate the maximum tensile stress in UTW due to both axle load and temperature differentials from the following equations.

$$\sigma_B^{UTW} = \frac{CPn(N.A.-c)}{I_B}\left[C_1 \log(\frac{l}{b}) + C_2 \frac{N.A.}{c} + C_3\right] \qquad \textbf{Eq. (3.26)}$$

$$\sigma_U^{UTW} = \frac{CnPc}{2I_U}\left[C_1 \log(\frac{l}{b}) + C_2 \frac{c}{h} + C_3\right] \qquad \textbf{Eq. (3.27)}$$

$$\sigma_T = CE_c \alpha \Delta T\left[C_4 \frac{c}{l} + C_5\right] \qquad \textbf{Eq. (3.28)}$$

Step 8. Obtain the stress ratio SR in the UTW and determine the maximum allowable number of load repetitions using the following equations.

$$SR > 0.55,\ N = 10^{12.1(0.972-SR)} \qquad \textbf{Eq. (3.29-a),}$$

$$SR > 0.45,\ N = \left(\frac{4.258}{SR-0.4325}\right)^{3.268} \qquad \textbf{Eq. (3.29-b)}$$

Step 9. If the UTW fatigue criterion indicates a smaller number of ESALs than W_D, increase the UTW thickness and repeat Steps 4 to 9.

Step 10. Choose the final UTW thickness by comparing bond and unbond design process.

3.4 PCA Design Procedure

The Portland Cement Association design procedure was developed by the Construction Technology Laboratories, Inc. In order to develop this design procedure, a three-dimensional finite element method was used. The model was calibrated and verified from field data collected in Missouri and Colorado. The Three-dimensional Finite Element Method (3D FEM) was used in the correction of factors used in the Two-dimensional Finite Element Method (2D FEM) and, therefore to simplify the derived prediction equations. This collaboration procedure is explained in the following subsections.

3.4.1 Development of the 3D FEM

The model was developed using the NISA STATIC finite element package. A total of nine slabs were simulated in a 3 by 3 arrangement. Spring elements were used at the UTW joints to simulate load transfer and interface between the HMA and the UTW. In order to assess the sensitivity of the model inputs, a parametric evaluation was performed—including center and edge loading conditions with and without cracks—in the HMA layer (the fully bonded, partially bonded, and unbonded cases).

3.4.2 Verification of the 3D FEM

In order to verify the developed model, field data from Missouri and Colorado were used. The measured stresses in the UTW in unbonded slabs were approximately 14 to 34 percent higher than the fully bonded 3D FEM simulation. It should be noted that only one correction was made to the FEM model to account for partial bonding.

3.4.3 Development of a Modified 2D FEM and Prediction Equations

ILSL2 2D finite element program was used to simplify the development of the design procedure. Multiple linear regression was used to derive relationships between the measured response from the 2D and 3D models. The developed equations for the prediction of the responses are stated as follows:

$$\log_{10}(\varepsilon_{HMA,18kSAL}) = 5.267 - 0.927 \times \log_{10}(k) + 0.299 \times \log_{10}\left(\frac{L_{adj}}{l_e}\right) - 0.037 \times l_e \qquad \textbf{Eq. (3.30)}$$

$$\log_{10}(\varepsilon_{HMA,36kTAL}) = 6.070 - 0.891 \times \log_{10}(k) - 0.786 \times \log_{10}(l_e) - 0.028 \times l_e \qquad \textbf{Eq. (3.31)}$$

$$\log_{10}(\sigma_{PCC,18kSAL}) = 5.025 - 0.465 \times \log_{10}(k) + 0.686 \times \log_{10}\left(\frac{L_{adj}}{l_e}\right) - 1.291 \times \log_{10}(l_e) \qquad \textbf{Eq. (3.32)}$$

$$\log_{10}(\sigma_{PCC,36kTAL}) = 4.898 - 0.559 \times \log_{10}(k) + 1.395 \times \log_{10}\left(\frac{L_{adj}}{l_e}\right) - 0.963 \times \log_{10}(l_e) - 0.088 \times \left(\frac{L_{adj}}{l_e}\right) \qquad \textbf{Eq. (3.33)}$$

$$\Delta\varepsilon_{HMA,\Delta T} = -28.698 + 2.131 \times \alpha_{PCC} \times \Delta T + 17.692 \times \left(\frac{L_{adj}}{l_e} \right) \quad \textbf{Eq. (3.34)}$$

$$\Delta\sigma_{PCC,\Delta T} = 28.037 - 3.496 \times \alpha_{PCC} \times \Delta T + 18.382 \times \left(\frac{L_{adj}}{l_e} \right) \quad \textbf{Eq. (3.35)}$$

Where, $\varepsilon_{HMAC,18kSAL}$ is HMA bottom strain due to a 18-kip single axle load($\mu\varepsilon$), $\varepsilon_{HMAC,36kTAL}$ is HMA bottom strain due to a 36-kip tandem axle load($\mu\varepsilon$), $\sigma_{PCC,18kSAL}$ is UTW corner (top) stress due to a 18-kip single axle load(psi), $\sigma_{PCC,36kTAL}$ is UTW corner (top) stress due to a 48-kip single axle load(psi), $\Delta\varepsilon_{HMA,\Delta T}$ is Additional HMA bottom strain due to temperature gradient($\mu\varepsilon$), $\Delta\sigma_{PCC,\Delta T}$ is additional UTW corner (top) stress due to temperature gradient(psi), α_{PCC} is thermal coefficient of expansion of the PCC(ε/°F), ΔT is temperature gradient in UTW(°F), l_e is the effective radius of relative stiffness for fully bonded slab (inches), and L_{adj} is adjusted slab length(in), defined as:

$$L_{adj} = 12 \times (8 - 24/(L/12 + 2)) \quad \textbf{Eq. (3.36)}$$

where L is the joint spacing in inches.

3.4.4 Fatigue Model

The final step of the design procedure is to calculate the predicted fatigue damage. Fatigue of the PCC at the corner of the UTW and fatigue at the bottom of the HMA were considered as follows:

Fatigue of the PCC by PCA fatigue equation

$$\log_{10}(N_{PCC}) = \frac{0.97187 - SR}{0.0828}, \text{ for SR>0.55} \quad \textbf{Eq. (3.37)}$$

$$N_{PCC} = \left(\frac{4.2577}{SR - 0.43248}\right)^{3.268}, \text{ for } 0.45 \leq SR \leq 0.55 \quad \textbf{Eq. (3.38)}$$

Where N_{pcc} is the fatigue life for the PCC.

Fatigue damage of the HMA by the Asphalt Institute equation

$$N_{HMA} = 0.0795 \times \left(\frac{1}{\varepsilon_{HMA}} \right)^{3.29} \times \left(\frac{1}{E_{HMA}} \right)^{0.854} \quad \textbf{Eq. (3.39)}$$

Where NHMA is the fatigue life for asphalt concrete pavement.

Chapter 4. Conclusions

The performance of several thin whitetopping (TWT) projects shows some variation in distress type and distress level. In some projects, severe corner cracking was developed under the wheel paths on the driving lane. In other projects, cracking in the panels on the driving lane near the shoulder was more pronounced. Reflective and load related cracking was common on all projects. However, most projects provided over 5 years of satisfactory service before reconstruction was required.

Performance of the test sections in the Minnesota Department of Transportation (MnDOT) shows that joint spacing has a significant effect on performance. Corner cracking appears to be the primary failure mode, and fatigue cracking is believed to be the primary cracking mechanism. Analysis also shows that bonding is an important factor to the long-term performance of whitetopping.

Ultrathin whitetopping provides small joint spacing to minimize stresses from wheel load applications as well as temperature and moisture variations. However, joint locations relative to wheel load applications should be given significant consideration. In stress-reduction mechanism by bonding, debonding between concrete and asphalt layers always occurred near panel edges or cracks. The bond at the center of panels was found to be intact.

Based on the field evaluations, partially bonded systems should be assumed in whitetopping design procedure. Otherwise, the procedure might be under-predict the stresses and the performance of the whitetopping might be compromised. It is recommended that joint spacing for thin whitetopping pavement to be 6 feet in both directions. As for the load transfer at the joints, dowel bars at the transverse contraction joints are not critical for the performance based on the Colorado thin whitetopping test sections. However, long-term monitoring is needed to determine the effect of load transfer devices.

The review of existing design procedures for whitetopping indicates that there is a need for improvements, especially the wheel load stress levels in slabs with different joint spacing. Also to be included are the effects of environmental loading, such as zero-stress temperatures and subsequent temperature and moisture variations.

References

Winkelman, T. J., "Whitetopping Construction and Early Performance in Illinois," Construction Report, Physical Research Report No. 144, Illinois Department of Transportation, June 2002.

Burnham, T. R., "Forensic Investigation Report for Mn/Road Ultra-thin Whitetopping Test Cells 93, 94, and 95," Report No. MN/RC-2005-45, September 2005.

Nenad G., "Development of a Design Guide for Ultra-thin Whitetopping(UTW)," Report No. FHWA 2001-018, New Jersey Department of Transportation, November 1998.

Scott M. T., M. J. Sheehan, and P. A. Okamoto, "Guidelines for the Thickness Design of Bonded Whitetopping Pavement in the State of Colorado," Report No. CDOT-DTD-R-98-10, Colorado Department of Transportation Research, December 1998.

Matthew J.S, S.M. Tarr, and S. Tayabji, "Instrumentation and Field Testing of Thin Whitetopping Pavement in Colorado and Revision of the Existing Colorado Thin Whitetopping Procedure," Report No. CDOT-DTD-R-2004-12 Final Report, Colorado Department of Transportation Research, August 2004.

Wu, C. L., S. M. Tarr, T. M. Refai, M. A. Nagai, and M. J. Sheehan, Development of Ultra-Thin Whitetopping Design Procedure, Portland Cement Association, 1998.

Nishizawa, T., Y. Murata, and T. Nakagawa, "Curling Stress in Concrete Slab of Ultra-Thin Whitetopping Structure," Presented at the 81st Annual Meeting of the Transportation Research Board, Washington, D.C., Jan. 2002.

Nishizawa, T., Y. Murata, and K. Kokubo, "Mechanical Behavior of Ultra-Thin Whitetopping Structure Under Stationary and Moving Loads," *Transportation Research Record 1823*, Transportation Research Board, National Research Council, Washington, D.C., pp.102-109, 2003.